Journal of Neurocytology **31**, 211–229 (2002)

Chance or design? Some specific considerations concerning synaptic boutons in cat visual cortex

JOHN C. ANDERSON, TOM BINZEGGER, RODNEY J. DOUGLAS and KEVAN A. C. MARTIN*

Institute of Neuroinformatics, University of Zürich and ETH Zürich, Winterthurerstrasse 190, 8006 Zürich, Switzerland
kevan@ini.phys.ethz.ch

Received December 20, 2002; accepted January 8, 2003

Abstract

To understand the rules by which axons lay down their synaptic boutons we analyzed the linear bouton distributions in 39 neurons (23 spiny, 13 smooth) and 3 thalamic axons, which were filled intracellularly with horseradish peroxidase (HRP) during *in vivo* experiments in cat area 17. The variation of the total number of boutons and the total axonal length was large (789–7912 boutons, 12–126 mm). The overall linear bouton density for smooth cells was higher than that of spiny cells and thalamic afferents (mean $\pm$ sd, 110 $\pm$ 21 and 78 $\pm$ 27 boutons per mm of axonal length). The distribution of boutons varied according to their location on the tree. Distal axon collaterals (first and second order segments in Horton-Strahler ordering) of smooth neurons had a 3.5 times higher, spiny cells and thalamic afferents a 2 times higher bouton density compared to the higher order (more proximal) segments. The distribution of interbouton intervals was positively skewed and similar for cells of the same type. In most cases a γ-distribution fitted well, but the distributions had a tendency to have a heavier tail. To a first approximation these bouton distributions are consistent with both diffuse and specific models of interneuronal connections. Quite simple rules can explain these distributions and the connections between the different classes of neurons.

Introduction

The complexity of the cortical circuits led early investigators to see only tangled thickets, a random mesh of connections in which no specific cortical circuits were to be found (Cajal, 1989). Theories were developed based on the assumption that the patterns of connections of individual neurons were irrelevant and that the mass action of an aggregate of neurons was the key to understanding cortical function (Sholl, 1956; Freeman, 1975). Modern studies, beginning with Hubel and Wiesel (1962, 1972) have largely overturned this view in favour of highly specified and stereotyped connections between cortical neurons that are repeated over and over to generate a crystal-like cortical architecture (Szentágothai, 1975; Rockel *et al*., 1980). In the most recent models, the circuit has evolved such precise wiring that the specificity extends beyond simply connections between different types of neurons to the actual position of the connection on the postsynaptic neuron. On this view, the surface of each neuron is an intricate mosaic of specific synaptic connections made with select presynaptic partners (Somogyi *et al*., 1998; Dantzker & Callaway, 2000; Kozloski *et al*., 2001; Silberberg *et al*., 2002). The hope is that when all these synapses are mapped, and their stereotyped and specific 'weights' known, then the role of the different neurons in the circuit will be plain. Impressive as the achievements have been in deciphering the cortical circuits, there is far from unanimity as to whether one can define a 'canonical' cortical circuit. This is most evident in the cat visual cortex, where there has been a long-standing debate as to the form of the basic functional circuit. Following Hubel and Wiesel (1962, 1965), one view is that the cortical layers constitute levels of a feedforward pathway within which there is some elaboration of receptive field properties between input and output. Another view is that the circuits within and between layers are recurrent, and that this is an essential part of their function (Nó, 1949; Creutzfeldt, 1977; Douglas *et al*., 1995). However, in most cortices, the debate over the precise form of the circuits has yet to begin. Even in very intensively studied circuits of the rat barrel cortex, or cortical areas 3 and 17 of monkey, only fragments of the cortical circuit have been assembled.

* To whom correspondence should be addressed.

0300–4864

The discussion of the specificity of connections is pursued at quite different levels. The oft-cited epitome of specificity is the chandelier cell, which forms its synapses exclusively on the initial segment of pyramidal cells (Freund *et al*., 1983). Specificity of location is of course typical for all cell types: the chandelier cell is perhaps more extreme. However, at the next level the question remains unanswered as to whether the chandelier cell specifically 'selects' particular pyramidal cells or simply forms multiple synapses with the axon initial segment of any pyramidal cell it comes across. Clearly, there are aspects of cortical function, *e.g.* gain control, attentional modulation, where diffuse rather than specific connections may be necessary. Without knowing the computation, one cannot simply assume that all connections have equal specificity, in the sense in which it is usually meant. The axo-axonic cell is also at one extreme in selecting a single (albeit broad) class of neurons—the pyramidal cells. All axons have preferred targets, but in general they form synapses with many different types of neurons. For example, in early studies in the cat we discovered that thalamic afferents formed synapses with all types of neurons whose dendrites lay within the axonal field (Martin & Whitteridge, 1984; Freund *et al*., 1985b). The same is true of the thalamic afferents in the mouse barrel cortex (White, 1989).

Most neurons do form synapses with multiple types of neurons and multiple sites: with spines, dendritic shafts and somata and some non-chandelier cells also form synapses with the axon (Gonchar *et al*., 2002). However, the strongest case that can be made for the 'selective' targeting of synapses comes not from anatomical studies but from physiological studies of simple cells in layer 4 of cat primary visual cortex. Here cross-correlation studies indicate that the On and Off subfields of the simple cells reflect the input from On and Off center X-type thalamic afferents (Tanaka, 1983; Reid & Alonso, 1995). This spatial precision of the innervation of these axons must be very high in order to preserve the spatial resolution of the receptive field. To appreciate the problem of achieving such precision, one must realize that each point in layer 4 is covered by between 400–800 X-type afferents, half of which are On and half are Off center (Freund *et al*., 1985a). What is even more remarkable is that each neuron receives only between 1–8 synapses from each thalamic afferent (Freund *et al*., 1985b). Since each layer 4 neuron has several hundred thalamic synapses, this means that there is considerable convergence of the thalamic input to the individual cortical neuron. This is reflected in the scatter of LGN receptive fields that cover subfields of simple cells (Reid & Alonso, 1995). Nevertheless the spatial precision of On and Off subfields of the simple cells is impressive.

Discovering the rules by which neurons interconnect with such precision has very important consequences for models of the development of cortical networks. Although much effort has been devoted to studying cortical connectivity, we are still far from understanding the rules that generate these circuits. It is clear that the formation of any particular synapse requires that an axon grows to a particular target and forms a synaptic bouton at the appropriate location. The literature on the axon branching patterns of cortical neurons is largely anecdotal and the mechanism of the actual placement of boutons along the axon is not well understood. Analyses of fragments of Golgi-stained axons in the rodent neocortex have given the rather surprising result that the placement of boutons along individual axon collaterals is random, *i.e.* the interbouton intervals approximate an exponential distribution (Braitenberg & Schüz, 1991; Hellwig *et al*., 1994). The authors interpret this as indicating that the cortical wiring is 'essentially random'. Measurements of interbouton intervals in the cat (Martin & Whitteridge, 1984; Kisvárday *et al*., 1985, 1987; Friedlander & Martin, 1989) also give positively skewed distributions reminiscent of the rodent, but no attempts were made to identify the underlying generative process. Here we have attempted to define the type of process that generates the position of individual boutons along a branch of an axon and in so doing have extended the work pioneered by Braitenberg and Schüz (1991) in the rodent. In addition, we consider the issue of how specific connections can be achieved if boutons are laid down randomly along the axon collaterals.

Material and methods

PREPARATIONS AND MAINTENANCE OF ANIMALS

The neurons examined in this study were obtained from anesthetized adult cats that had been prepared for *in vivo* intracellular recording (see Martin & Whitteridge, 1984; Douglas *et al*., 1991, for details). All experiments were carried out by KACM and colleagues under the authorization of animal research licenses granted by the Home Office of the U.K. and the Cantonal Veterinary Authority of Zürich. We first recorded from each cat extracellularly and mapped the receptive field orientation preference, size, type, binocularity and direction preference by hand. The mapping was repeated intracellularly and horseradish peroxidase (HRP) was then ionophoresed into the cell. Thalamic afferents were classified as X or Y-type using a battery of tests (Friedlander & Stanford, 1984; Martin & Whitteridge, 1984). After appropriate survival times, the brains were fixed and processed to reveal the HRP and osmicated and embedded in resin to eliminate differential shrinkage. Shrinkage of the tissue was estimated to be 11%. The block of tissue containing the intracellularly filled neurons was serially sectioned in the coronal plane at a thickness of 80 μm. This processing allowed the material to be examined at both the light and the electron microscope level.

CELL RECONSTRUCTIONS

Neurons were reconstructed in three dimensions with the aid of a light microscope (Leitz Dialux 22) with drawing tube

attachment magnified to $\times 400$ attached to an in-house 3D reconstruction system (TRAKA). TRAKA was written in PASCAL by RJD and Danie Botha. The reconstructions were characterized by a list of data points and stored for further usage. Each data point consists of a code describing the digitized structure (axon or bouton) and its three spatial co-ordinates and thickness (where relevant). The axonal arborisations are complex and often extend through many histological sections. The measurement error of the digitized structures was estimated by measuring four boutons ten times. The standard deviation was smaller than 0.6 μm in all 3 dimensions. The data was rotated in order to bring all reconstructed cells into the same coordinate system.

AXON AND BOUTON REPRESENTATION

For technical reasons occasional axonal collaterals of a given cell could not be connected to the main tree and were ignored in this analysis. Each data point consists of a code describing the structure digitised, its three spatial co-ordinates and its thickness. The boutons are assumed to represent the major presynaptic location of synapses. They are represented by points in the 3D space, and the axonal and dendritic collaterals by open polygons. The locations of the boutons were digitised together with the axons. So each bouton is linked to its source collateral, and this data organisation permits us to study the distribution of the boutons along the collaterals.

The boutons do not always lie exactly on the route of the axon as represented by the digitised polygon. Trivially, the boutons may lie away from the polygon because physically extended structures such as the axon are digitised as points and lines, which have no thickness. Moreover, there are small measurement errors in the digitisation process. The third, and biologically relevant, reason for displacement of the boutons away from the axon is the existence of terminaux boutons. These are spine-like boutons connected by a small stalk, or neck, to the axonal shaft. In order to analyse sequences of boutons on axonal branches projected the measured points (boutons) onto the axonal polygon (Fig. 1).

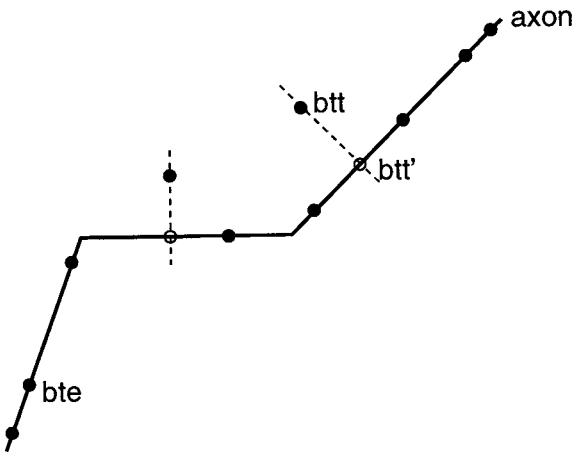

Fig. 1. Representation of an axon. The reconstruction of an axonal branch is represented by a polygon in the 3D space. Boutons on the axon are represented by filled circles. En passant boutons (bte) sit directly on the axon, while terminaux boutons (btt) are displaced and had to be projected onto the axon (btt', open circles). We analysed the sequence of bte and btt' along the axon.

DENDROGRAMS

A dendrogram of a tree is a 2D diagram that represents the branching behaviour of the tree. Each branch point is represented by a horizontal line, which links the parent branch to its daughter branches. The length of this line is arbitrary and is chosen to be long enough to avoid intersections with other branches. The branches (also axon collaterals) themselves are represented by vertical lines and their length is proportional to the measured length of the branch. We also superimposed the locations of boutons (projected onto the branches) onto the dendrogram. It is a property of the dendrogram that all its intersections with the same horizontal have the same displacement from the origin of the tree, when the distance is measured along the shortest axonal path from an intersection to the origin of the tree.

Horton-Strahler ordering scheme

In order to investigate the distribution of boutons on different parts of the axonal tree, we assigned each axonal collateral an order. We used the method proposed by Strahler (Strahler, 1957, see Fig. 2). Each collateral in a binary tree is given an order in the following way: the end collaterals (*i.e.* the collaterals with no children) have all order 1. If the two children of a collateral have order k, the collateral is assigned order $k+1$. If one child has order k and the other an order smaller than k, the collateral is assigned to the larger order k. Each maximal path formed by consecutive collaterals of the same order k is called a *segment* of order k. This ordering scheme is intuitively best understood in terms of pruning. If all order 1 collaterals (the end-collaterals) are removed, a tree remains whose end-collaterals are the order to segments of the old tree.

Interbouton interval

For each bouton of the first or second order segments the length of the interbouton interval ('ibi') to the neighbouring

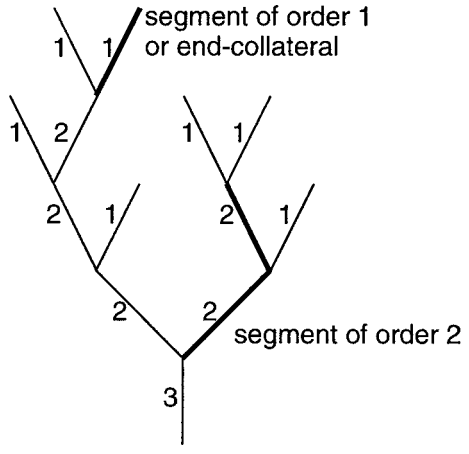

Fig. 2. Ordering scheme used to describe the collaterals of a binary tree. Each number indicates the 'Horton-Strahler order' of a collateral. By definition each end collateral (one is indicated in bold) has order 1. Collaterals with children of similar order k have order $k+1$. Collaterals with children of different orders k_1 and k_2 have order $\max(k_1, k_2)$. A 'segment' of order k is a maximum chain of collaterals of this order. A segment of order 2 is indicated with a bold line.

bouton closer to the root was determined. If no such neighbour existed, the interval to the beginning of the point of the segment was taken. Histograms of interbouton intervals (bin size 1.5 μm) were fitted by a γ-distribution $f_{\alpha,\nu}$ with 'scale' parameter $\alpha > 0$ and 'shape' parameter $\nu > 0$, defined by $f_{\alpha,\nu}(x) = \frac{1}{\Gamma(\nu)}\alpha^{\nu}x^{\nu-1}e^{-\alpha x}$, where $\Gamma(\nu) = \int_0^{\infty} t^{\nu-1}e^{-x}\,dt$ is the gamma function. For the fit with the histograms only distances were used that were smaller than $d = i \cdot 1.5 - 0.75$, where i is the first bin for which the bins i and $i + 1$ contain no distances. The best fit was found by minimising the least square error with the Levenberg-Marquardt method (*e.g.* Press *et al.*, 1997). The quality of the fit was assessed using the Kolmogorov-Smirnov test (significance level 0.01). Two sets of ibi's were tested to be significantly different (significance level 0.01) by comparing their median using the bootstrap method (Efron & Tibshirani, 1993, p. 221).

Poisson process with dead zones

A stationary Poisson process with dead zones (Cox & Isham, 1980) was used to explain the interbouton interval distributions (Fig. 11A). First a Poisson process with rate λ ($\lambda > 0$) was created. The increments of this point process follow an exponential distribution h_λ with mean $1/\lambda$. A distance $\tau > 0$ (dead zone) from a distribution g_d was chosen. Then beginning with the first point of the Poisson process, all following points of the Poisson process were deleted until the resulting interbouton interval was larger than τ. With the selection of a new τ and going on with the next point of the Poisson process, this procedure was repeated many times. It can be shown (Cox & Isham, 1980) that the increments of the new point process are independent of each other and have a common distribution f_o which is the convolution of g_d with h_λ. For simplicity we use $g_d = f_{\lambda,\nu_d}$ with arbitrary $\nu_d > 0$. In this case it is $f_o = f_{\lambda,\nu_d+1}$ (Feller, 1971, p. 47).

Results

An analysis was made of 39 neurons whose axons arborized in area 17 of the cat. Figure 3 shows the position and type of these neurons, whose arborizations were found in all layers. Figure 4A shows a reconstruction of a layer 4 spiny stellate neuron, which forms its principal axonal arborization in layer 4. Its axon formed five distinct clusters of boutons, including a cluster around the dendritic arbor. In the dendrogram of this (Fig. 4B) and the following axons, the thin vertical lines indicate the length of the axon collaterals, the branches, and the position of each bouton is indicated by a dot. The horizontal lines are drawn only to connect the collaterals and represent the branch points.

For comparison with the spiny stellate neuron shown in Figures 4A and B, we illustrate the arbors and dendrograms of the major types of neurons that also made their principal arborizations in layer 4. The lateral geniculate neurons arborise mainly in layer 4. One such arbor of a Y-type thalamic neuron is illustrated in Figure 4C with its associated dendrogram in Figure 4D. It formed 7 clusters of which all were contained in layer 4.

The thalamus provides about 5% of the asymmetric synapses in layer 4 (Garey & Powell, 1971; Winfield & Powell, 1983; LeVay, 1986; Ahmed *et al.*, 1994). By comparison with the thalamic afferents, the layer 6 pyramidal cells provide almost 10-fold more excitatory synapses in layer 4 (Ahmed *et al.*, 1994). The axonal arborization of one of these layer 6 neurons is shown in Figures 5A and B. Unlike the Y-axon, which had an additional small collateral projection to layer 6, this layer 6 neuron arborised exclusively in layer 4 where it formed six distinct clusters of boutons.

The axons of the spiny stellate, layer 6 pyramid and thalamic neurons all form asymmetric synapses in layer 4. The symmetric synapses in layer 4 are provided by the smooth GABAergic neurons, which are typically small basket cells (Fig. 5C and D). The axon arbors of the small basket cells of layer 4 are quite different from the axon arbors of the excitatory neurons in being very much more compact and in being nearly confined to a single cluster. The change in the scale of the illustration of the basket cell also indicates that compared to the three types of excitatory axon illustrated in Figures 4 and 5, the inhibitory axon formed many short branches, densely studded with boutons.

BOUTON DENSITY

Global density

The total number of boutons varied greatly for the different cells, between 789 and 7912 (mean $\pm$ std: 3554 $\pm$ 1729, Fig. 6A). Even for cells of the same type the bouton number can vary by a factor of at least three (*i.e.* the pyramidal cells of layer 2/3 or layer 6). In contrast, other cell-types, such as the basket cells in layer 2/3, have very similar bouton numbers.

The total length of an axon has a similar variation for the different cells (41 mm $\pm$ 21 mm, range 12–126 mm, Fig. 6B). It seems likely that the variation in bouton number and that of the axonal length are correlated: the more axon a cell has, the more boutons can be formed on it. A regression analysis shows that this is indeed the case for the smooth cells ($r = 0.90$), Fig. 6B). The correlation is worse for the spiny cells and thalamic afferents ($r = 0.79$). For example the layer 6 pyramidal cells that project to layer 4 (p6(L4)) have as high a number of boutons as the pyramidal cells in layer 2/3 (p2/3), but their total axonal length is much shorter.

For a given total axonal length the smooth cells typically have a higher number of boutons on the axon than the spiny cells and thalamic afferents (Fig. 6B). As a consequence the ratio of the two numbers (*i.e.* the 'overall' bouton density) is higher for the former group (110 $\pm$ 21 boutons per mm) than for the latter (78 $\pm$ 27 boutons per mm).

Bouton density on different tree segments

Inspection of the dendrograms in Figures 4 and 5 shows that the boutons are not uniformly distributed on the

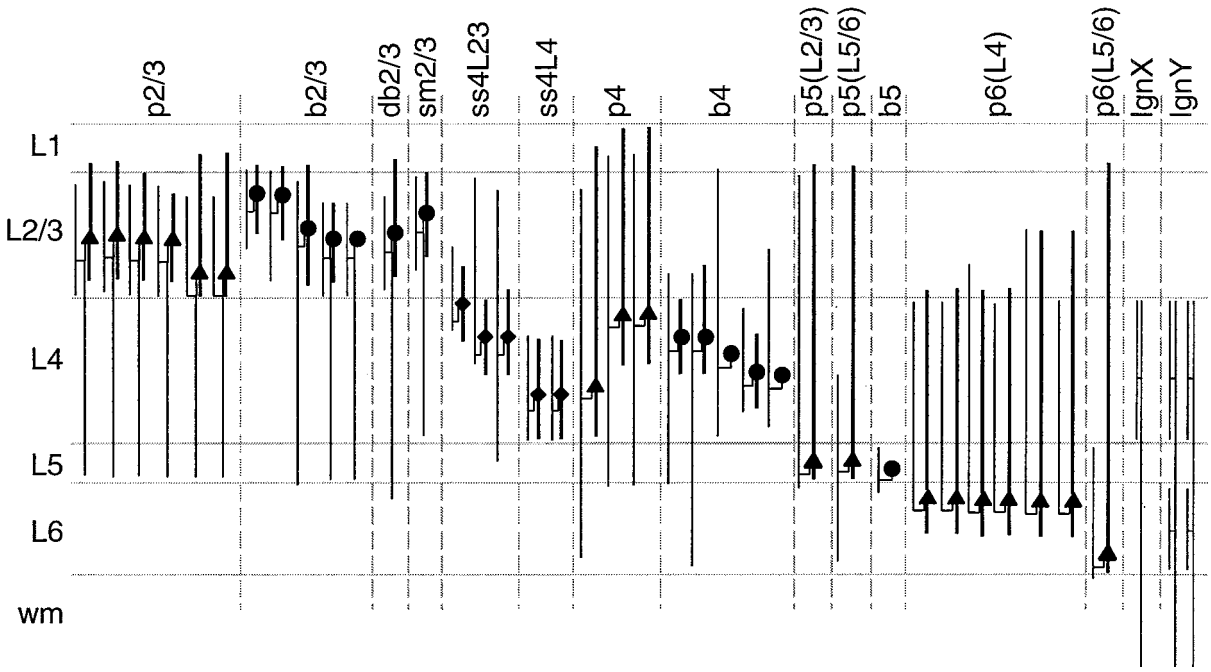

Fig. 3. Schematic representation of soma position and vertical range of axons and dendrites of reconstructed cells. Soma is indicated by a dot (smooth cell), triangle (pyramidal cell) or square (spiny stellate cell). For the thalamic afferents no soma was drawn. Thick vertical lines indicate dendrites, thin vertical lines axons. Horizontal lines indicate the lamina borders. The position of the somata within a layer reflects the approximate true position. Similarly, the extent of the vertical lines within a layer reflects the true vertical range that was covered by the axonal and dendritic trees. wm: white matter. Top labels indicate the cell-types. b2/3, b4, b5: Basket cells in layer 2/3, 4 and 5. db2/3: double bouquet cell in layer 2/3. sm2/3: An unclassified smooth cell in layer 2/3. p2/3, p4, p5, p6: pyramidal cells in layer 2/3, 4, 5 and 6. Pyramidal cells in layer 5 and 6 were further distinguished by the preferred layer of the axonal innervation (p5(L2/3), p5(L5/6), p6(L4) and p6(L5/6)). ss4: spiny stellate cells in layer 4 with major axonal projection to layer 2/3 (ss4(L2/3) or to layer 4 (ss4(L4)). lgnX and lgnY: thalamic afferents of type X and Y.

axonal tree. The axons tended to have their boutons located on the first and second order segments (*i.e.* on the distal collaterals), while the higher order segments were often only sparsely dotted with boutons. In fact, the overall bouton density of the first and second order segments was on average 127 $\pm$ 23 boutons per mm for the smooth cells and less for the spiny cells and thalamic afferents (86$\pm$ 28 boutons per mm). The overall bouton density for the higher order segments was for the smooth cells 36 $\pm$ 27 boutons per mm and higher for the spiny cells and thalamic afferents (43 $\pm$ 27 boutons per mm).

From now on we will consider the boutons on the first and second order segments only. This is only a minor restriction because these segments carry most boutons and form most of the total axonal length (Fig. 6A). On average they form 92% $\pm$ 5% (the first order segments alone 66% $\pm$ 8%) of the boutons and 82% $\pm$ 6% (the first order segments 55% $\pm$ 7%) of the axonal length.

The typical number of boutons on the first order segments was smaller for the smooth cells than for the spiny cells, while the relation was reversed for the typical bouton density (Fig. 6C and D). This is possible if the first order segments are smaller for the smooth cells than for the spiny cells. Comparison of the dendrograms in Figures 4 and 5 and inspection of the dendrograms of the other cells confirms this is so (not shown).

For the smooth cells, the typical bouton density of the second order segments tended to be smaller than that of the first order segments, although the total number of boutons on the segments was roughly similar (Fig. 6C and D, *e.g.* b2/3 and b4). In contrast, the typical bouton number for the spiny cells tended to be bigger for the second order segments than for the first order segments, but in many cases the typical bouton density was equal (Fig. 6C and D, *e.g.* p2/3 or p6L(5/6)). Again, both patterns are possible if the second order segments are longer than the first order segments.

INTERBOUTON INTERVALS

Median of interbouton intervals

The analysis of a large number of axon branches from the major morphological classes of cortical neurons and LGN afferents, indicated that there was considerable variation in the length of the interbouton intervals ('ibi'). However, in some cases the distributions

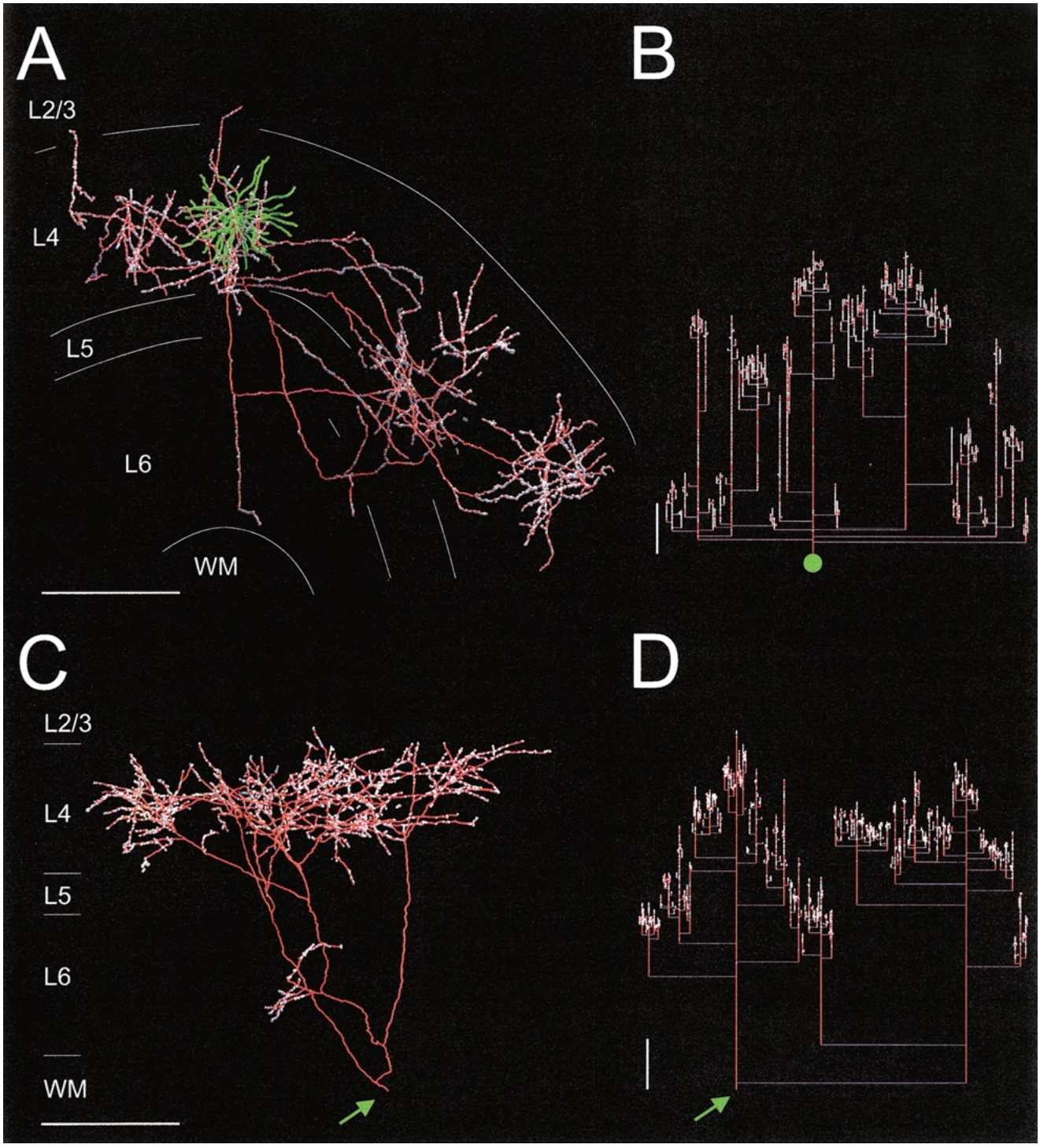

Fig. 4. Coronal view of reconstructed neurons and the dendrogram of their axonal trees. For this and the following figure the axon is indicated in black, axonal boutons in green, dendrites in red and cortical layer borders in gray. A: Spiny stellate cell in layer 4. Receptive field (RF) type, ocular dominance (OD) and size were as follows. Directional S1 ('simple') RF, OD 1, size 0.8 $\times$ 0.5 deg. B: Dendrogram of the spiny stellate cell shown in A. C: Y-type thalamic afferent. D: Dendrogram of the thalamic afferent shown in C. Scale bars: 500 μm.

correlated with the cell type. Median values of ibi varied considerably for the first and second order segments, between 3.6 μm and 10.6 μm (Fig. 7A), depending on the cell class. Smooth cells, with the exception of the double bouquet cell in layer 2/3 had small median ibi, on average 5.9 $\pm$ 0.9 μm. The spiny cells and thalamic afferents tended to have larger median ibi, on average 7.4 $\pm$ 1.6 μm. However, the bouton density can change along the axonal tree (Fig. 6C and D). We also wanted to know if the distributions of ibi are different for

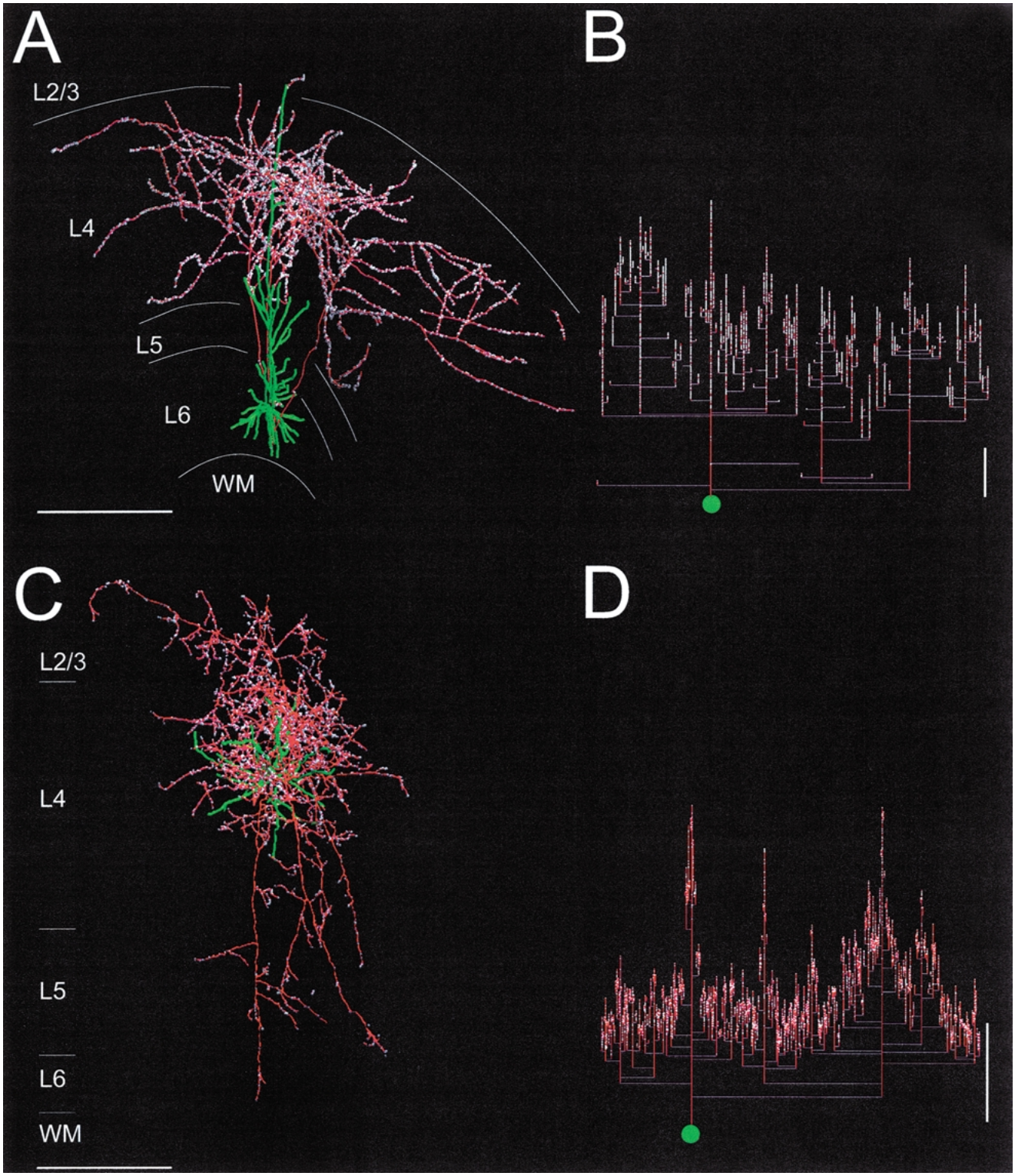

Fig. 5. Coronal view of reconstructed neurons and the dendrogram of their axonal trees. A: Pyramidal cell in layer 6. Directional S1 RF, OD 7, size 0.5 × 1.1 deg. B: Dendrogram of the pyramidal cell shown in A. C: Basket cell in layer 4. OFF-center RF, OD 7, size 0.2 × 0.2 deg. D: Dendrogram of the basket cell shown in D. Scale bar in A and B: 500 μm, in C and D: 250 μm.

different parts of the axon. First we compared the median values of ibi between boutons located either on the first or second order segments (Fig. 7A). In general the medians are rather similar (absolute difference $<2\ \mu$m) and only for 10/39 cases the difference was significant (gray bars in Fig. 7A). In particular the median ibi of the second order segments of smooth cells (7/13) showed a tendency to be significantly bigger. Smooth neurons

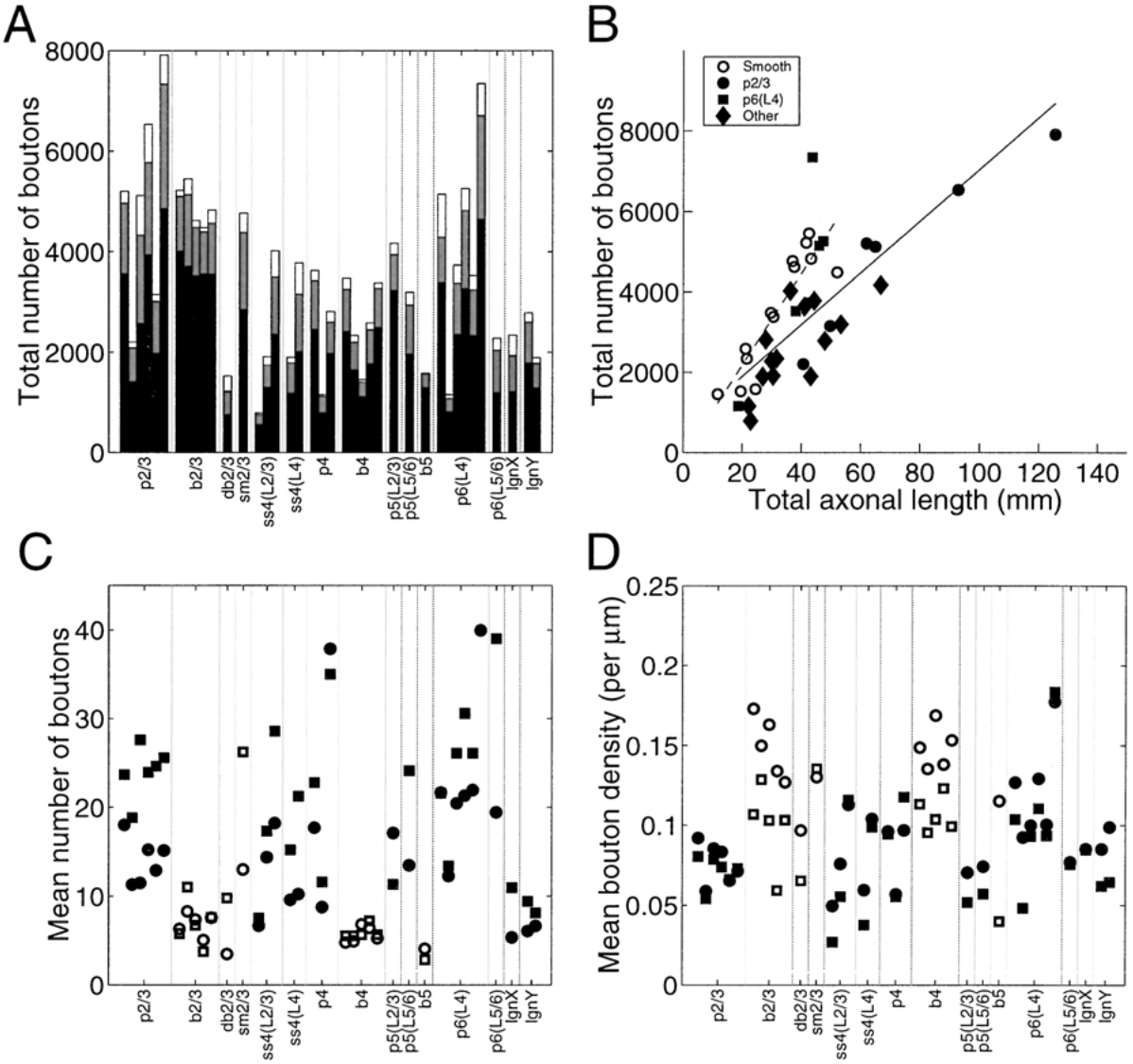

Fig. 6. Absolute number and density of boutons along the axonal trees. A: Each bar indicates the number of boutons on the axon of a reconstructed neuron. The contribution of the first order segments is shown in black, of the second order segments in gray and the higher order segments in white. B: Correlation between the total number of boutons and the summed length of the tree collaterals for each neuron. Stippled line indicates regression line through the smooth neurons (open dots, correlation coefficient $r = 0.90$, slope $b = 113.54$), solid line through the spiny neurons and thalamic afferents (closed dots, $r = 0.79$, $b = 64.36$). C: For each neuron the mean number of boutons on segments of order 1 (circles) and order 2 (squares) were computed. D: For each neuron the mean bouton density on segments of order 1 (circles) and order 2 (squares) were computed. C and D: Open symbols indicate smooth neurons, filled symbols spiny neurons and thalamic afferents.

also showed a tendency to have a lower bouton density on the second order segments (Fig. 6D).

Next we compared the median values of ibi on different subtrees of an axon. We considered all subtrees whose new root is segment order 4 in the tree. These subtrees correspond to the major branches of the axon. Each cell have between 2 and 21 of these subtrees, corresponding to the number of dots in Figure 7B. The number of ibi investigated for the different subtrees ranged between 39 and 1723 (331 ± 280). For each subtree we determined the median ibi of the order 1 segments, which are also the order one segments of the tree. The medians were scattered around the median of the whole tree. The range of the subtrees median ibi was typically smaller for smooth cells (1.5 ± 2.5 μm) than for spiny cells and thalamic afferents (2.1 ± 2.4).

For 19/39 neurons, the were at least two subtrees with significantly different ibi, 8/13 smooth cells and 10/23 spiny cells and one of 3 thalamic afferent. Because many subtrees contributed all their boutons to a single cluster, we were able to compare the ibi's of subtrees that formed either proximal or distal clusters. No clear pattern emerged.

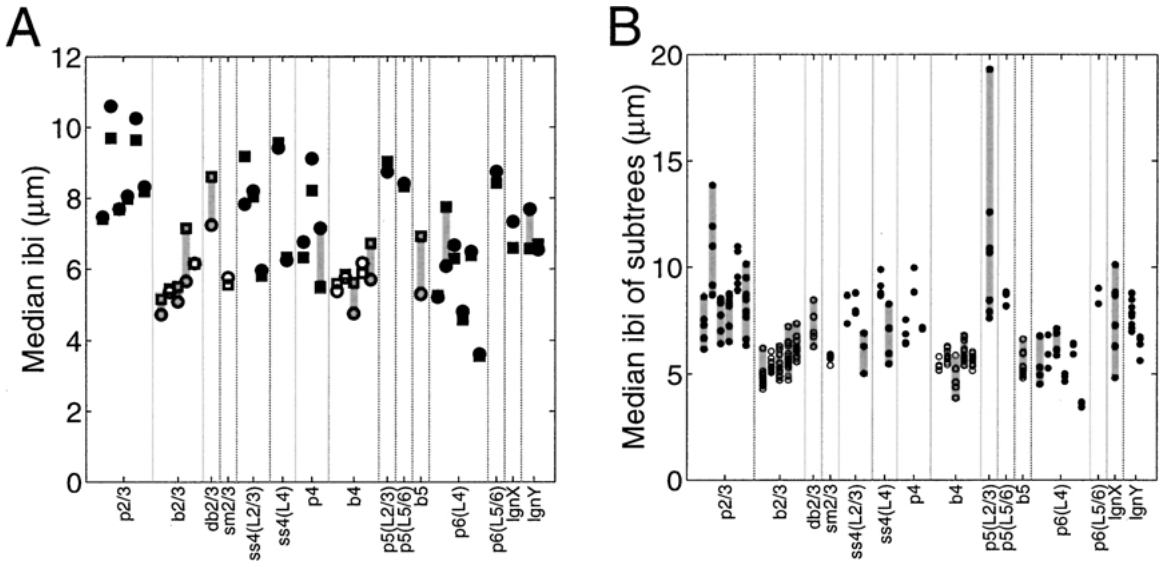

Fig. 7. Median of interbouton intervals (ibi) on different parts of the tree. A: Median ibi for boutons located on first order segments (circles) and on second order segments (squares), shown for each neuron. Filled segments indicate spiny neurons and thalamic afferents, open symbols indicate smooth neurons. Gray bars indicate neurons with significant differences of median ibi. B: Median ibi of first order segments which were all connected to the same order 4 segment. Each dot in a vertical column indicates the median ibi for the different subtrees of a neuron. Gray bars indicate neurons for which at least two subtrees had significant differences of median ibi.

Histogram of interbouton intervals

The histograms of ibi (bin size 1.5 μm) were positively skewed for all cells (Fig. 8). The distributions within a class tended to be similar and we therefore grouped the histograms by their cell-types. Cell types with similar distributions were pooled again and we finally came up with four distinct groupings of the histograms of ibi. The main difference between the distributions of the different groups is the location and height of the peak. The first group (Fig. 8A) is made of layer 4 projecting pyramidal cells in layer 6. Typically, the distribution of these cells had their maximum in the first bin. The layer 6 pyramidal cell whose axon was restricted to layer 6 had a totally different distribution. Like the remaining spiny cells, which formed a second group (Fig. 8B), this cell had a flatter distribution. The cells in this second group had a tendency to have fewer very small ibi, so that the peak of the distribution was not in the first bin but in the second or third. For the third group (Fig. 8C), the thalamic afferents, the lack of small ibi is even more pronounced for all three members. The last group (Fig. 8D) was formed by the smooth cells. For these cells (except for the double bouquet cell and one of the basket cells in layer 4, indicated by thin lines in the inset), the lack of small distances was pronounced and the distributions were very steep.

Fit of exponential and γ-distributions to the histograms

In fitting of the histograms, extreme distances were taken as outliers and were eliminated from the analysis of the histograms. Specifically, ibi greater than a threshold distance d were not included, where d was the value of the first bin in the histogram of ibi for which the bin and its successor contained no entries.

We attempted to fit the histograms with a γ-distribution with shape parameter ν and scale parameter α (see Methods). Examples of fits to histograms of ibi on first order segments which did not deviate significantly are shown in Figure 9A. The fit deviated significantly only for 8/39 neurons for (3 smooth cells, 3 spiny neurons and 2 thalamic afferent). Even if the deviation was significant, the fit was still a reasonable approximation (Fig. 9B). For many of these worse fits the number of small ibi (between 3 and 4.5 μm) was underestimated by the fitted curves (*i.e.* black dots in Fig. 9B).

Figures 9C and D show the estimated parameters for the histogram of ibi on first order segments. The shape parameter ν of the γ-distribution was for many cells close to 1 (Fig. 9C) which suggests that an exponential distribution could be fitted as well (an exponential distribution with mean m is a γ distribution with $\nu = 1$ and $m = 1/\alpha$). This was indeed the case for 5 of the 6 layer 4 projecting pyramidal cells in layer 6, and also for a spiny stellate cell, a layer 4 pyramidal cell and the deep projecting layer 5 pyramidal cell.

A comparison of the estimated parameters for the fitted γ-distributions to the ibi on second order segments shows little variance. The average absolute differences of the ν values was 0.2 ± 0.2, for the α values it was 0.03 ± 0.03. Only 4 spiny cells had a fit that deviated

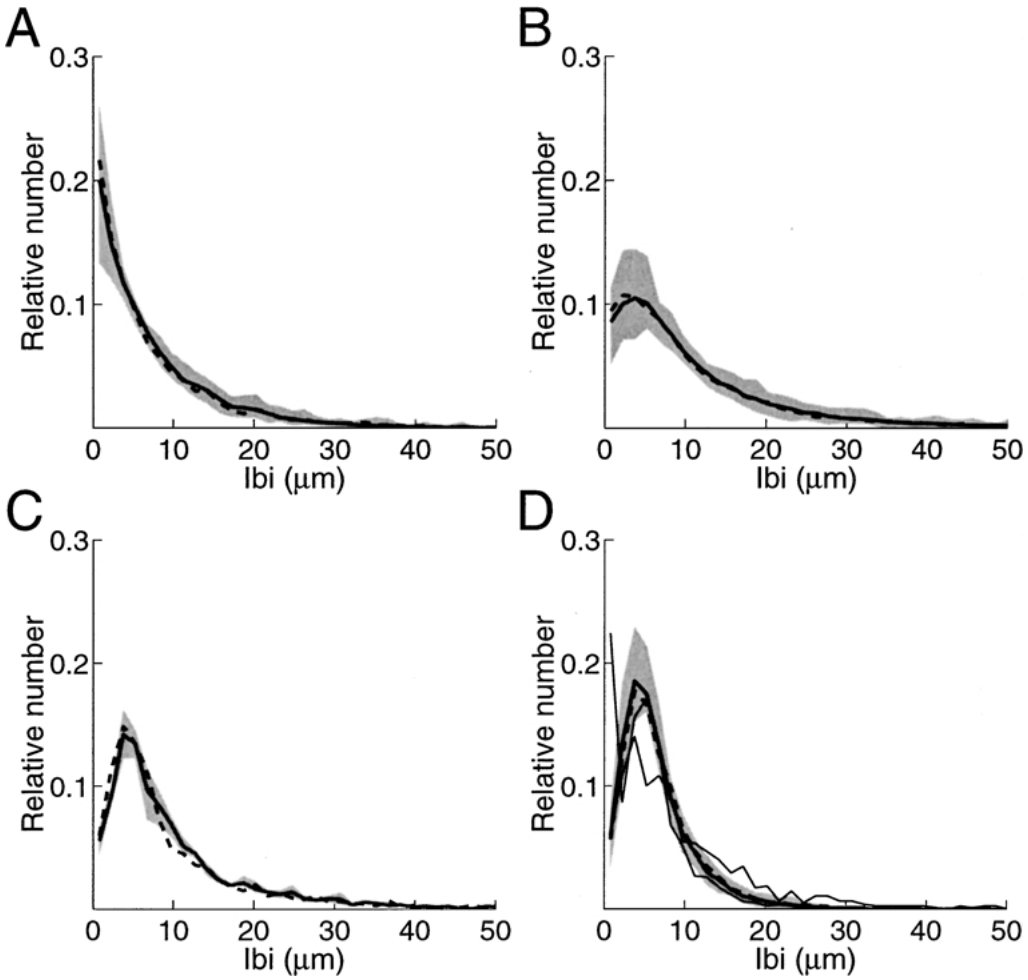

Fig. 8. Histogram of interbouton intervals of axonal trees grouped by cell-type and similarity. Four groups were formed corresponding to the four histograms in A–D. The bold solid line indicates the histogram of the pooled ibi of first order segments of each group. The upper border of the shaded area indicates the bin-wise maximum and the lower curve the bin-wise minimum of the individual histograms of ibi on first order segments. The bold stippled line indicates the histogram of the pooled ibi of second order segments of each group. Bin size was 1.5 μm. A: Pyramidal cells in layer 6 with an axonal projection to layer 4. Median of pooled ibi is 5.0 μm (first order segments) and 4.7 μm (second order segments). B: Remaining spiny cells in area 17. Median of pooled ibi is 7.9 μm (first order segments) and 7.8 μm (second order segments). C: Thalamic afferents. Median of pooled ibi is 7.1 μm (first order segments) and 6.6 μm (second order segments). D: Smooth cells. The thin lines indicate a basket cell in layer 4 and a double bouquet cell in layer 2/3. These two cells were excluded from the following statistics. Median of pooled ibi is 5.5 μm (first order segments) and 5.8 μm (second order segments).

significantly from the histogram. For 7/13 smooth cells the fitted γ-distribution of the ibi on the first order segments were significantly different from the histogram of the ibi on the second order distribution. Two of the 3 thalamic afferents had significant differences in median ibi, but only 5/23 spiny neurons showed this difference. This demonstrates again that the spiny neurons are more similar in their bouton distribution between first and second order segments.

If the exponential distribution fitted well to the ibi on first order segments (discussed above) it also fitted well to the distribution of ibi on the second order segments. There were 4 additional neurons which had a significantly good fit on the second order segments but not for the first order segments.

A MODEL FOR BOUTON PLACEMENT

Poisson process

The analysis of mouse axons by Braitenberg and Schüz indicated that boutons are placed randomly along axonal branches, *i.e.* that the boutons on all collaterals are placed according to the same (homogeneous) Poisson process (Braitenberg & Schüz, 1991; Hellwig *et al.*, 1994). The model was applied to cells of the mouse and rat cortex, but they supposed it to be a general rule for cortex. Our analysis of the axonal trees indicates that the bouton density and the interbouton intervals change with the location of the collateral on the tree (Figs. 6 and 7). Randomness, by contrast, implies that all collaterals form about the same density of boutons.

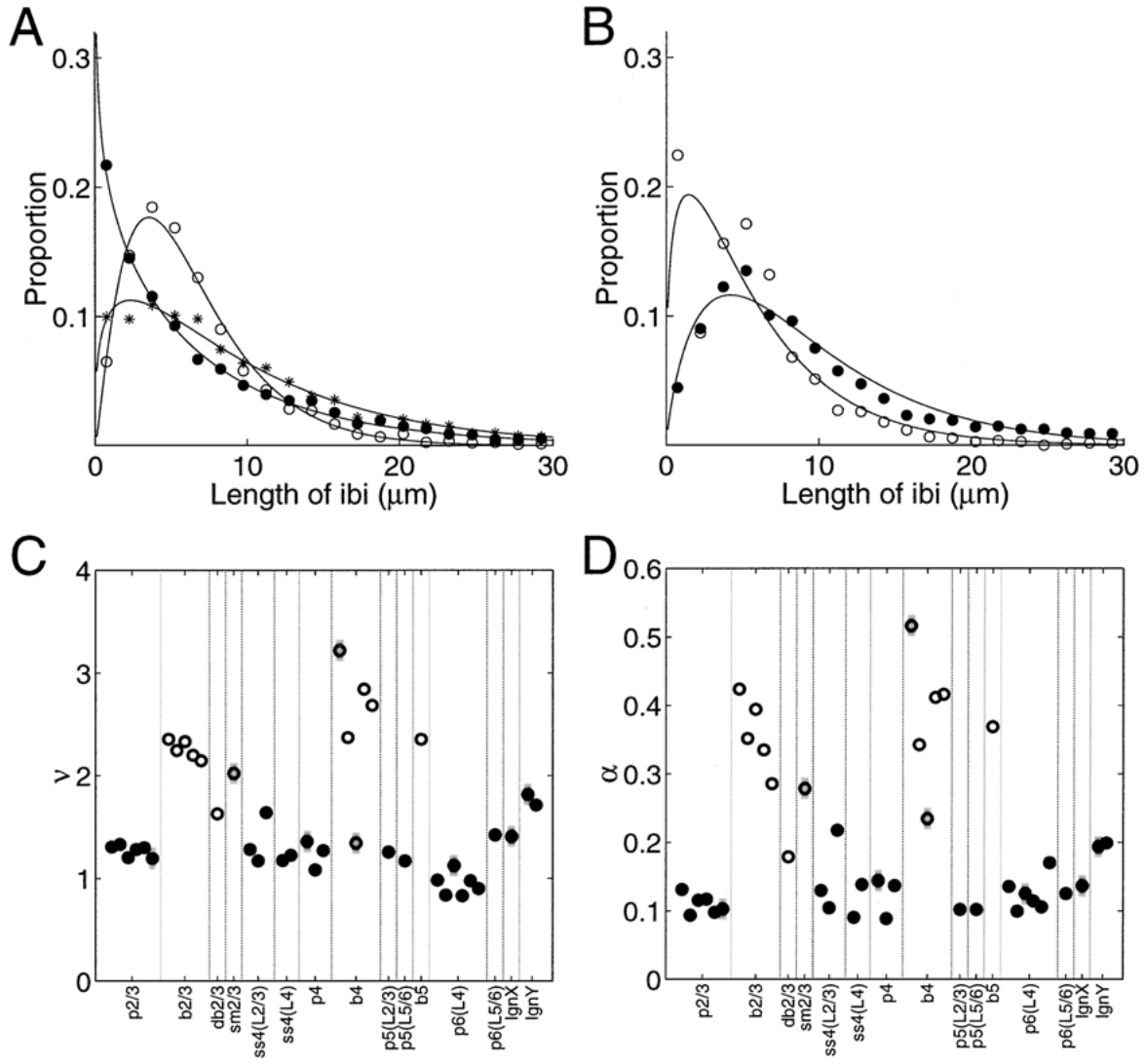

Fig. 9. Fit of γ-distribution with shape parameter ν and scale parameter α to the histogram of ibi on first order segments. Gray bars indicate neurons for which the fitted curve deviated significantly from the histogram. A: Three representative examples of histograms and the fitted γ distributions (solid lines), a basket cell in layer 2/3 (open dots, estimated parameters $\nu = 2.25$, $\alpha = 0.35$), a pyramidal cell in layer 6 (closed dots, $\nu = 0.83$, $\alpha = 0.11$) and a pyramidal cell in layer 2/3 (stars, $\nu = 1.31$, $\alpha = 0.13$). The fit did not deviate significantly. B: Examples of histograms of ibi on first order segments for which the fitted curves (solid lines) deviated significantly. Open dots indicate a basket cell in layer 4 (fitted parameters $\nu = 1.34$, $\alpha = 0.23$, closed dots a thalamic afferent ($\nu = 1.82$, $\alpha = 0.19$). C and D: Estimated parameters ν (C) and α (D) of the fitted γ-distributions to the histograms of ibi on first order segments. Closed dots indicate spiny cells and thalamic afferents, open dots smooth cells. A–D: In fitting the histograms, large distances were ignored. Specifically, ibi greater than a threshold distance d were not included, where d was the value of the first bin in the histogram of ibi for which the bin and its successor contained no entries. Bin size 1.5 μm.

However, the Poisson model could be true for certain sub-regions on the tree.

We can test the random hypothesis by modeling bouton placement by a Poisson process. We can place the first bouton on the collateral and then ask, at what distance from this bouton is the next bouton to be formed? This distance is drawn from an exponential distribution. After the second bouton is formed, another distance is drawn from the exponential distribution to place the third bouton and so on. By construction, the interbouton intervals have to be exponentially distributed. Based on the Kolmogorov-Smirnov test, some of the distances of boutons on first and second order segments in our samples were indeed distributed in that way. However, most (70–80%) were not. An obvious reason for mismatch with the exponential distribution is the lack of small distances.

Most spiny cells have a mix of terminaux and en passant boutons along their axons. The relative proportions of each bouton type are shown in Figure 10, which indicates that most spiny cells have less then 30% boutons

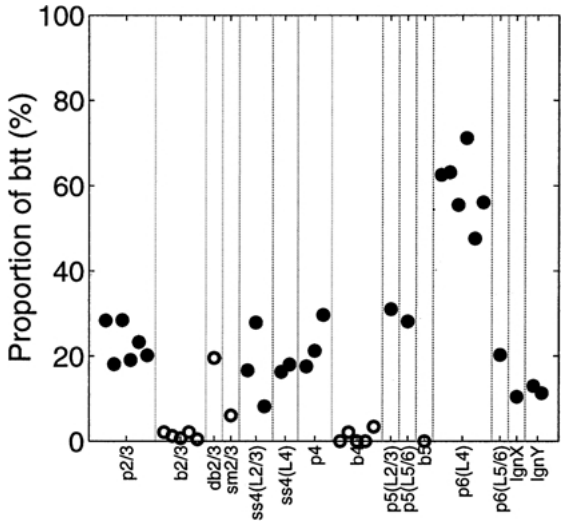

Fig. 10. Proportion of terminaux boutons on an axonal tree. Open dots indicate smooth cells, closed dots spiny cells and thalamic afferents. Boutons located at the end tips of the first order segments were not counted as terminaux boutons.

terminaux on the axonal tree. The exceptions are the layer six pyramidal cells that project to layer 4 that bear many bouton terminaux ($59 \pm 8\%$, range 48–71%). A similar observation for the layer 6 pyramidal cells was previously made (McGuire *et al.*, 1984; Martin & Whitteridge, 1984). In addition it was found that en passant boutons were most common for the thalamic afferents and star pyramidal cells (McGuire *et al.*, 1984; Martin & Whitteridge, 1984; Freund *et al.*, 1985a; Ahmed *et al.*, 1997) and that for a layer 3 and layer 5 pyramidal cell the axon bore with both types of boutons (Martin & Whitteridge, 1984; Kisvárday *et al.*, 1986). We found that individual cells have small variations in the distributions of the two bouton types. For example the absolute percentage differences of boutons en passant is smaller than 15% for first and second order segments. The terminaux boutons could form small ibi, because their spine-like necks can curve to bring the boutons themselves in close proximity to one another (Fig. 1). However, our method of plotting the boutons would tend to produce small ibi artificially.

It is easy to see how the Poisson process could be modified to allow for a lack of small distances in the ibi distribution and still maintain the notion of random placement of boutons. A very simple example of such a model is shown in Figure 11A. It is assumed that the boutons are produced by a Poisson process so that the ibi are distributed by an exponential distribution with rate $\lambda > 0$. For simplicity of the argument we assume that the length of the dead zones is a γ-distribution with scale parameter λ and shape parameter ν_d. When the first bouton is produced, a length of a dead zone is randomly selected from the γ-distribution. All boutons which were created by the Poisson process within that

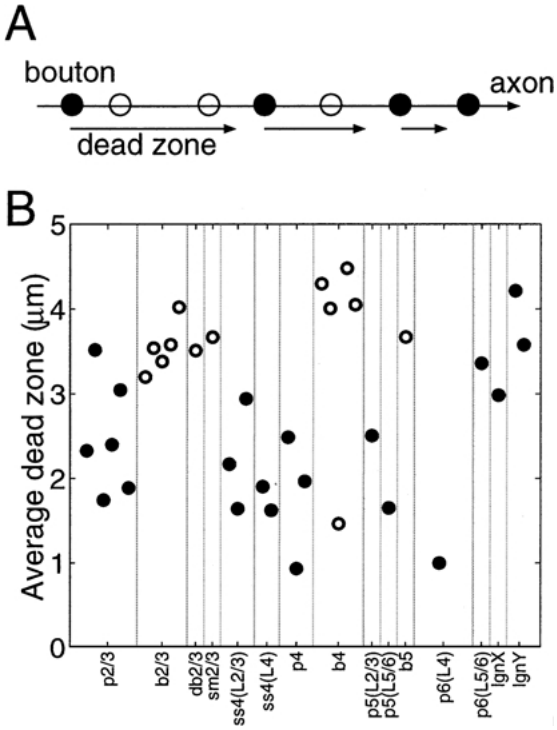

Fig. 11. Poisson process with dead zones. A: Illustration of a Poisson process with dead zones. Shown is an axon (horizontal line) on which boutons (open and closed circles) are formed, starting from the left. The open circles indicate boutons which would have been formed by the Poisson process, but were prevented from being formed by the introduction of a dead zone (arrows). The sample of closed circles are the boutons that are finally observed on the axon. Dead zones are drawn from a γ-distribution. B: Estimated average length of dead zones. Open dots indicate smooth cells, closed dots spiny cells and thalamic afferents. Cells for which the estimated dead zone is negative are not shown.

dead zone are ignored (Fig. 11A). The distribution of ibi of the resulting process is a γ-distribution with scale parameter λ and shape parameter $\nu_d + 1$ (see Methods). Thus, based on the estimated parameters α and ν for the histogram of ibi (Fig. 9C and D), we get for the parameters of the dead zone $\lambda = \alpha$ and $\nu_d = \nu - 1$. We applied this dead zone model to cells with $\nu > 1$ (Fig. 9C) and computed the average dead zone length ν_d/λ (Fig. 11B).

If we identify the dead zones with bouton diameters, the predicted average bouton diameter is, ignoring the layer 6 pyramidal cells that project to layer 4, between 0.9 and 4.5 μm (Fig. 11B). For cells in cat V1 and thalamic afferents, estimated bouton diameters range between 0.5 μm and 3 μm (Kisvárday *et al.*, 1985; Gabbott *et al.*, 1987; Ahmed *et al.*, 1994, 1997).

Long tails

In the analysis of the ibi distributions and variations across the axons, we noted the existence of large ibi, which we designated as outliers according to a

threshold distance d (see above). For the different cells, d ranged for first and second order segments between 21 μm and 83 μm. The number of intervals discarded was less than 10% of the total number of ibi on either the first or the second order segments. In previous studies of basket cells (Kisvárday *et al.*, 1985, 1987) large ibi were also noted. In order to determine the mean of the layer 4 basket cells, all ibi larger than 20 μm (8% of all ibi) were ignored and for the layer 5 basket cell ibi larger than 30 μm (7%) were ignored. The large ibi were mainly placed on the main axonal trunk where the boutons are sparsely distributed. However, we also found large ibi on first and second order segments. The maximal ibi for each cell on these segments was between 31 μm and 1315 μm.

We investigated the nature of the large ibi more closely by means of the empirical survivor function, $S(x)$, which is defined as the proportion of ibi larger than x (abscissae in Fig. 12). One such distribution is shown (in log-log space) in Figure 12A. The ibi were taken from the pooled sample of second order segments pooled from the 5 basket cells in layer 2/3. The survivor function $S_\gamma(x)$ of the best fit to the pooled ibi is shown as a comparison. As can be observed, for large ibi the empirical survivor function is above the survivor function of the γ-distribution, indicating that the γ-distribution underestimates the probability of the occurrence of large ibi. This is also true for most ibi on first and second order segments of individual cells. For smooth cells, the two survivor functions ($S(x)$ and $S_\gamma(x)$) started to separate for ibi larger than 10 μm (15.4 $\pm$ 4.0 μm), for spiny cells and thalamic afferents it is for ibi larger than 13 μm (25.0 $\pm$ 7.6 μm). The proportion of ibi larger than this threshold ranges between 0.8% and 36% (10.9 $\pm$ 7.4%) of all the ibi either on first or on second order segments.

The empirical survivor function of the ibi in Figure 12A approximates in log-log space a straight line indicated by the approximately constant slope for values of 15 μm $< x <$ 50 μm in Figure 12B. This means that for large ibi the survivor function is proportional to $x^{-\beta}$ for soma positive β($\beta = 2.6$ in Fig. 12B) and for large x. A linear region could also be found for other neurons. However, in general the linear part was smaller and the variance of the slope within the linear region was higher than for the basket cells illustrated in Figure 12.

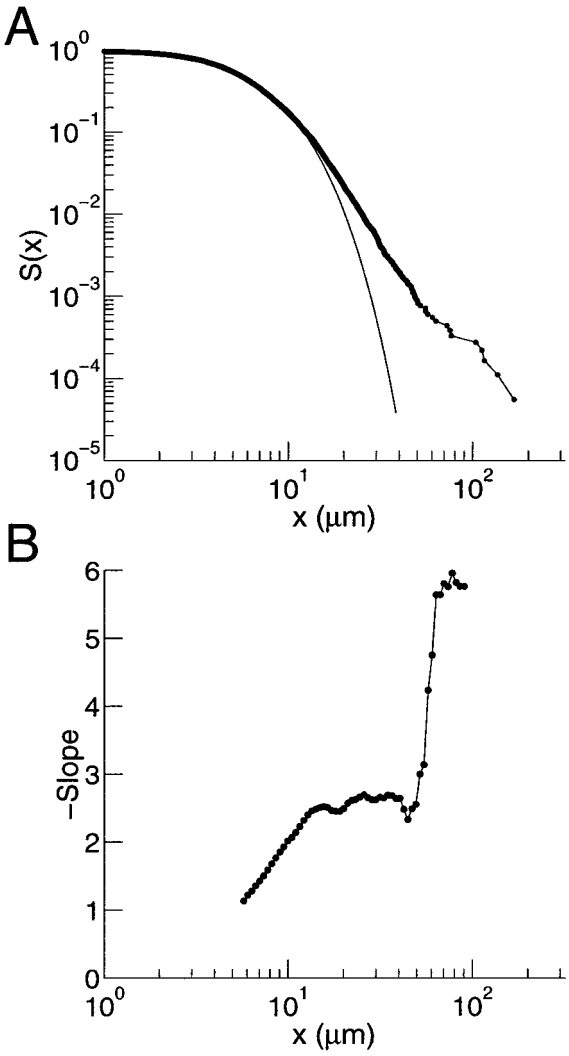

Fig. 12. The long tail behaviour of the bouton distribution of basket cells in layer 2/3. A: The empirical survivor function $S(x)$ (in log-log space) of the pooled ibi of second order segments. In addition we fitted a γ-distribution to the histogram of ibi ($\nu = 2.1, \alpha = 0.3$). Its survivor function $S_\gamma(x)$ is indicated (continuous line). For the fit large ibi were ignored. B: Estimated local slope of $S(x)$ as a function of x. The local slope was estimated by moving a window of size 0.5 along the x-axis in log-log space and calculating the slope of the regression line through the piece of curve $S(x)$ determined by the window.

Discussion

The question posed by Hellwig *et al.* (1994) is whether the boutons are distributed randomly along the axons. The question was answered by them in the affirmative: 'We may not be too far from the truth when we say that the distribution of synapses along the axons looks as if it had rained synapses on the axons' (Braitenberg & Schüz, 1991, p. 58). Similar metaphors were used in their analysis of Golgi-stained axons of pyramidal cells in mouse cortex (Hellwig *et al.*, 1994). They claimed that a single Poisson process described the distribution of interbouton intervals. Similar long tailed distributions appear in previous descriptions of individual axons from thalamic afferents and various cell types in cat visual cortex (Martin & Whitteridge, 1984; Kisvárday *et al.*, 1985, 1987; Tettoni *et al.*, 1998; Friedlander & Martin, 1989). In the present study we explored in a far larger sample of different neurons, the suitability of applying a Poisson process to our data. Our analysis indicates that this is at best an approximation, which

in some cases is quite poor. Tettoni *et al.* (1998) fitted their distributions of ibi in callosal axons after eliminating distances >25 μm, to extract the maxima. Their fitted function was proportional to a γ-distribution with shape parameter $\nu = 2$, but they did not report on the goodness of the fit.

Different axonal segments

At the present time we have little idea what controls the size of axonal arbors or the number of synaptic boutons they form. However, evidence for changes in the bouton density for different parts of the axon was detected for all cell types studied. The changes can often be correlated with the location of the bouton in the cortex. Obvious examples are the lamina specificity of the axonal arbors, *e.g.* the layer 6 pyramidal cells that project to layer 4 and tend to avoid forming synapses in layer 5 and 6 (Fig. 5A). But also within a layer the formation of boutons can change. Boutons formed infrequently on an axon before it branched to form a distal cluster (Fig. 4A). This last observation can also be seen as the prominent preference of the boutons to be located on the end collaterals (first order segments) of the axonal tree. The end collaterals, which make up 55% of the total length of the axonal tree, bear, on average, 66% of the total number of boutons. Similar trends were reported for the callosal axons in the cat (Tettoni *et al.*, 1998) where the end collaterals of callosal axons formed 33% of the total axonal length but bore 71% of the boutons. Hellwig *et al.* (1994) (see also Braitenberg & Schüz, 1991, p. 55) found no evidence that the bouton density was higher on the peripheral parts of the axonal trees of mouse pyramidal cells. However, they reconstructed the segments of axons in 2-dimensions and selected only some of the longest collaterals (>150 μm) or those that carried more than 30 boutons for analysis. It is clear that the entire tree should be analysed because of the variations in density that occur within a single tree.

Influence of cell type

Cells of similar type tend to have similar bouton density and interbouton interval distributions. Median ibi on distal collaterals (*i.e.* first and second order segments) covered a range between 3 μm and 11 μm (Fig. 7A), which presumably reflects some rule governing the connection of the different cell types to their targets. Spiny cells and thalamic afferents tend to have larger median ibi than smooth cells. A basket cell axon in layer 4 forms a bouton about every 5 μm , whereas for the spiny stellate cells it is only about every 8 μm. There are two previous studies in which typical ibi of smooth cells in cat area 17 were determined. For a layer 4 basket cell the mean ibi was 6.4 μm (Kisvárday *et al.*, 1985), which is in agreement with our findings (mean ibi between 5.4 and 7.7 μm on first and second order segments) and for

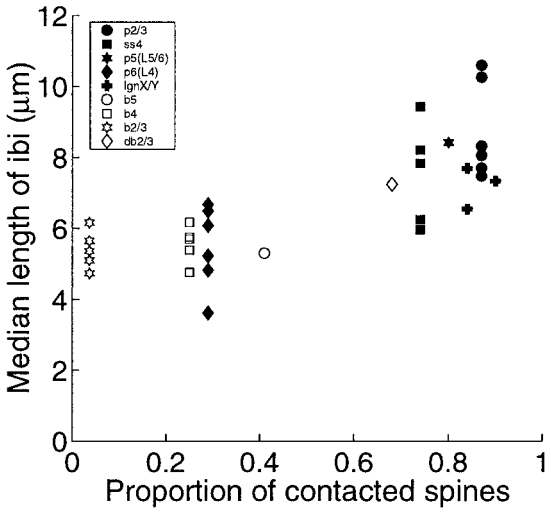

Fig. 13. Correlation between median length of ibi on an axonal tree and the proportion of spines that the tree contacted. Estimates of the proportion of spines contacted were taken from the literature (Kisvárday *et al.*, 1986; Freund *et al.*, 1986; Tamás *et al.*, 1997, 1998; Somogyi & Cowey, 1981; Anderson *et al.*, 1994; Somogyi *et al.*, 1983; Kisvárday *et al.*, 1985, 1987; McGuire *et al.*, 1984; Somogyi, 1989; Garey & Powell, 1971; Freund *et al.*, 1985a).

a basket cell in layer 5 the mean was 9.4 μm (Kisvárday *et al.*, 1987). For this cell we found a mean ibi of 7.5 μm on first order segments and 11.3 μm on second order segments. For interbouton intervals of thalamic afferents of the cat (or kitten) visual cortex (area 18, layer 4A) the mean ibi was 11.2 μm (Friedlander & Martin, 1989). Again, this is in good agreement with our values (mean ibi between 9.5 μm and 12.8 μm on first and second order segments).

The basket cells, spiny stellate cells and thalamic afferents all have layer 4 spiny cells as their major targets. The basket cells, which have small ibi, form many synapses with cell bodies and proximal dendritic shafts, whereas the spiny stellate cells and thalamic afferents target dendritic spines and have larger ibi. The correlation of median ibi with target type was supported by other cell types in our sample, as Figure 13 shows. From the same figure one can also see a tendency for the interbouton intervals to correlate with the layer of the soma. Layer 6 pyramidal cells have a smaller ibi than the spiny stellate cells in layer 4 or the pyramidal cells in layers 2 and 3. However, the same correlation does not seem to hold for smooth cells. There is clearly large variance even within the same cell class and for boutons within the same layers. For example, in layer 4 the median ibi for one layer 6 pyramidal cell was 3.6 μm while for another it was 6.7 μm. The study of Hellwig *et al.* (1994) of the ibi of 20 different pyramidal cells in the mouse cortex indicated a similar variance. The mean ibi varied between 2.2 to 7.0 μm. The source of the variation has not yet been identified.

Form of distribution

The distribution of ibi reveals a further difference in bouton formation. All ibi distributions are positively skewed, but display differences for very short distances. Some cells show a lack of small ibi while others do not. The lack of small ibi was especially pronounced for the smooth cells and the thalamic afferents, while it was less pronounced for superficial pyramidal cells and was absent for layer 6 pyramidal cells which project to layer 4 (Fig. 8). A lack of small distances was also reported in the study of the basket cells in layer 4 and 5 (Kisvárday *et al*., 1985, 1987) and for spiny cells (Martin & Whitteridge, 1984). Tettoni *et al*. (1998) found that the maxima of their fitted function occurred at 4.3 μm, which makes them more similar to thalamic afferents. In the mouse (Braitenberg & Schüz, 1991; Hellwig *et al*., 1994) the shortest distances are the most frequent, whereas the intrinsic axons across the visual areas V1, V2, V4 and 7a in the monkey lack small distances (Amir *et al*., 1993).

A lack of small distances can be interpreted as the existence of a 'dead zone', *i.e.* a small neighbourhood that is formed on the axon around each bouton in which no other bouton can be formed. The existence of a dead zone can be understood if one remembers that the boutons are physical objects of about 0.3 to 3 μm in diameter on an axonal branch of about 0.1 μm diameter. En passant boutons form beads along the trajectory of the axons, whereas the terminaux boutons are located on spine-like process that project a few microns from the axis of the axon. In the case of the en passant boutons, which are the most common, it follows that the centre of two boutons can never be closer than their diameter. Indeed, the estimated dead zones are of this order (≤ 5 μm). However, other effects such as limitations given by the growth mechanisms for boutons, or some metabolic constraints could also play a role.

The large ibi in the distribution of neurons (Fig. 12) indicate the occurrence of large gaps between neighbouring boutons. These large gaps are not captured by the Poisson process with dead zones and show the limitation of this model. There are many possible sources large gaps, one being that neurons that are to be contacted by an axon collateral are spaced by a distance corresponding to these gaps. For example, it is evident from reconstructions of thalamic axons (Gilbert & Wiesel, 1983) that there exist different periodicities of clustering. The large patches of boutons that form the ocular dominance columns are spaced at approximately 0.5 mm intervals. However there are also smaller clusters within these larger patches. These microclusters, which are also seen in the axonal arbors of the small basket cells of layer 4, are spaced about 100 μm apart (Kisvárday *et al*., 1985). Clusterings of different repeat intervals are also common in neurons lying outside layer 4 (Gilbert & Wiesel, 1983; Martin & Whitteridge, 1984) and these would contribute to the large interbouton intervals.

Neurons form mainly en passant boutons in making their synapses. The exception is the type of layer 6 pyramidal cell that projects to layer 4, which have a high proportion of terminaux boutons ($62 \pm 8\%$, see also McGuire *et al*., 1984; Martin & Whitteridge, 1984). Compared to other spiny neurons, the layer 6 neurons make smaller ibi on average. Although this may be partially an artifact of the method of projecting the bouton onto the shaft of the axon in order to make the interval distribution, it might also in part be due to the geometry of the spine-like stalks that can bring the terminaux boutons in close proximity to each other. A similar correlation was observed by Martin and Whitteridge (1984). They compared the interbouton intervals between rows of en passant boutons and rows of boutons terminaux (at least 5 in a row). Their study showed that the terminaux boutons formed more small distances than the en passant boutons. The reasons for this remain unclear, particularly as a recent study (Anderson & Martin, 2001) found no difference in the target type (spine vs. dendritic shaft) for the two bouton types.

An active role of the postsynaptic targets themselves are rarely considered in discussions of bouton formation. However, it is clear that the targets could themselves contribute to forming specific connections. We now know that dendritic spines can be generated *de novo* (Muller & Connor, 1991; Maletic-Savatic *et al*., 1999; Engert & Bonhoeffer, 1999) and thus they could provide a means whereby the dendrites themselves can be active in capturing specific passing axons. Such specificity would be largely invisible from the presynaptic side. The actual site of the synapse on the target cell may also have some influence on axonal morphology and bouton density. From reconstructions of layer 4 spiny stellate and basket cells, we know that basket cells provide a strong synaptic input to the soma and proximal dendritic shafts of spiny stellate cells, while the synapses from spiny cells are located more distally on the dendritic spines and shafts. If individual basket cells have to make their multiple synapses with a spatially restricted domain of their target neurons (*e.g.* the soma and proximal dendrites), this may require either more branches or the ibi interval to be as small as possible. Among the spiny cells, the layer 6 pyramidal cells also have small ibi. However they do not form multiple synapses with their targets (McGuire *et al*., 1984) so the close proximity of their boutons does not reflect multiple inputs to single cells, but may reflect the density of suitable targets in the neuropil. These observations remind one that we know very little about the environment within which axons are distributing their boutons. Studies of the ultrastructure of a volume of neuropil are totally lacking. It is also clear that a knowledge of the three dimensional distribution of the boutons of single

cortical cells is also an essential part of solving the puzzle of cortical circuits.

IMPLICATIONS FOR RULES OF CONNECTIVITY

The analysis of these axons shows the rich variety of ways in which the different cell types distribute their synaptic boutons along the axons. In seeking for the underlying rules one central consideration has been the manner in which the boutons distribute themselves along the axon. The strong claim made by Braitenberg and Schüz (1991) is that the concept of a 'terminal arbor' is meaningless because cortical pyramidal cells distribute their synaptic boutons diffusely over the whole tree. Braitenberg and Schüz (1991) observed that the absence of periodicity in the spacing of synapses implied that the axon has no rule whereby it decides where and when to form a synapse with possible targets in the surrounding neuropil. They supposed that the location of synapses was decided by the surrounding dendrites in the neuropil, which offer the axons postsynaptic sites. They argue that because the network of dendrites is 'to all intents and purposes 'random' the wiring of the cortex is also essentially random. The alternative, as they saw it, is that the cortical wiring is complicated beyond reason (Braitenberg & Schüz, 1991).

The data and analysis presented above, leads us to a rather different interpretation. Different cell types have characteristically different bouton distributions, even when they form their boutons in the identical volume of neuropil, as in the case of the axons projecting to layer 4 for example. Multiple factors were found to correlate with the bouton distribution, such as the layer of origin of the axon, the layer of termination, whether the parent cell was smooth or spiny, and even whether the boutons were en passant or terminal. The axons do not have a diffuse distribution of boutons over the whole tree, but instead have specific laminar targets and form clustered projections within those target lamina. This means that significant lengths of axon do not bear boutons or only sparsely. Thus, the appealing notion offered by Hellwig *et al*. (1994) that the distribution of boutons can be characterized by a single Poisson process with one rate parameter (synapses per unit length), does not apply to the present data.

However, even when reasonable fits to a Poisson process are found, this implies nothing about the specificity of the connections, as Braitenberg and Schüz (1991) acknowledged. A simple illustration of how the same axon with boutons distributed by a Poisson process could generate either random or specific connections is illustrated in Figure 14. In this example, the axons take a straight trajectory through the neuropil, as is observed in many axons of spiny cells. In the case of random wiring, a given axon traverses the neuropil and probabilistically forms synapses with any dendritic tree it encounters in the neuropil. If the location of the target neuron is distributed by a Poisson process, the interbouton intervals will be exponentially distributed (Fig. 14C, filled dots). In the converse case, where the axon forms its synapses selectively with a specific class of cells, the same exponential distribution of interbouton intervals will be achieved if the class of target neurons is distributed by a Poisson process. In the example illustrated, the axon still travels in a straight trajectory and forms synapses whenever it encounters a member of the specific class of neurons. Thus despite the specificity of connections, the resultant histogram of interbouton intervals is indistinguishable from the random case.

Although this is a hypothetical example for the purposes of illustration, it points out some important issues. One is whether different classes of neurons are distributed by a Poisson process. The answer is a clear 'yes' in the only instance where it has been examined. Winfield *et al*. (1981) examined the form of distribution of the Meynert cells of monkey area 17. The Meynert cells are a particularly convenient example for this purpose, because the cells are readily distinguishable with conventional histological methods, they occur in a single monolayer, and are of low enough density that the position of every cell can be plotted. Winfield *et al*. found that the nearest distance distribution of the Meynert cells was similar to that of a spatial Poisson process. It is thus not unreasonable to suppose that different classes of cortical neurons are distributed in the same manner. It is as if the different classes of cells lie suspended in a sea of neuropil, each class forming different densities of Poisson distributions at different depths.

Our hypothetical example shows that if the rule required any neuron to connect to specific individual neurons, rather than any member it encountered of a specific class, then the axon could not take a straight trajectory, but would have to twist and turn to make connections with specific neurons even if the neurons were organized in a geometric grid. Axons of cortical neurons (including the Meynert cells, Rockland & Knutson, 2001) are not highly contorted in general, which is consistent with our proposal that the specificity lies in connections between classes of neurons rather than between specific individual neurons. By allowing the axons to take relatively straight trajectories, such a rule of connectivity greatly contributes to optimizing the length of axon required to make a given set of connections (Peters & Kaiserman-Abramof, 1970; Swindale, 1981; Mitchison, 1991; Cherniak, 1992; Anderson & Martin, 2001).

The relatively short median interbouton intervals we observe implies that if an axon forms its synapses with only one class of neurons, then the members of that class must occur at relatively high density. The experimental evidence, however, indicates that most neurons form synapses with multiple classes of neurons

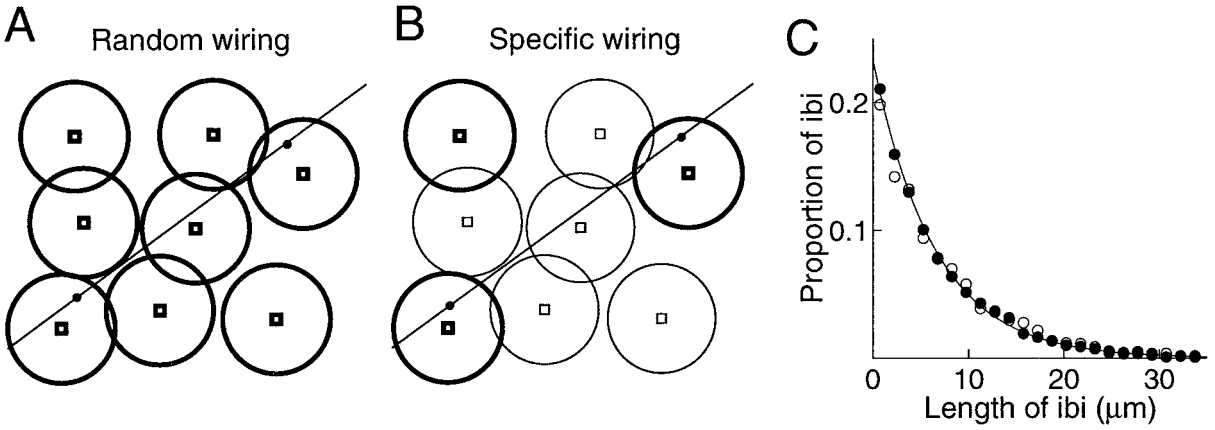

Fig. 14. Connectivity models showing that random and specific connectivity rules can both result in an exponential distribution of interbouton intervals. A and B: Formation of synapse between an axon and the dendritic field of a cells. The axon is indicated by a straight line, the cell-body by an open rectangle and the borders of the dendritic field by a large circle. The synapse is located on a bouton (filled circle). The possible locations of the bouton are restricted to the axonal segment that lies within the dendritic field and we assume that each of these locations is equally probable. For clarity the diagrams of A and B do not show the realistic densities of neurons used in C, hence the large interbouton interval. A: Random wiring. An axon (straight line) forming synapses with cells in a patch of cortex. Cell bodies in the patch are indicated by rectangles, their dendritic fields by large circles. Whenever an axon traverses a dendritic field, there is a probability p that the axon formed a synapse only with this cell. In this case the axon formed two boutons. Depicted is the situation with $p < 1$, *i.e.* the axon formed a single synapse only with some (2) of the possible 4 targets. B: Specific wiring. An axon (straight line) forming synapses with a predefined subgroup of cells (bold rectangles and large circles) in a patch of cortex. Whenever the axon traverses the dendritic field of a cell of this subgroup, a synapse is formed. The axon does not form synapses with the remaining cells in the patch (indicated by thin rectangles and large circles). C: Simulation of the distribution of interbouton intervals for the two wiring scenarios described in (A) and (B). A three dimensional patch of cortex in layer 4 of cat V1 with volume 300^3 μm^3 was modelled. The total number of cells in this patch is 1485 (Beaulieu & Colonnier, 1983). We assumed the location of the cell-bodies to be distributed by a Poisson process within this patch. The dendritic field was modelled as a sphere with radius 100 μm. 100 straight axons were laid through the patch, the formation of boutons was simulated, the interbouton intervals determined and pooled. In scenario (A), we assumed a selection probability of $p = 0.1$. The histogram of interbouton interval is indicated by closed dots. Also shown is the fitted exponential distribution to the data (continuous line, parameter $\alpha = 6.4$). In (B) we assumed that the subgroup contained 148 cells which were also distributed by a Poisson process. The histogram of interbouton intervals is indicated with open dots.

(Kozloski *et al.*, 2001). If these classes are all distributed by a Poisson process, then the resultant bouton distribution would still be exponentially distributed. The number of synapses made by one neuron on another will depend on the density of the axonal boutons and the target cells. Estimates based on random connectivity give binomial distributions whose means lie within the ranges seen experimentally (Freund *et al.*, 1985b; Braitenberg & Schüz, 1991; Douglas *et al.*, 1995; Feldmeyer & Sakmann, 2000).

The simple rule of specificity for classes of neurons rather than particular neurons would not exclude specificity at a finer grain. For example a rule could be that the synapses be formed with spines rather than dendritic shafts. The hypothesis also allows for a coarser level of specificity, as is evident in the vertical interlaminar connections or the horizontal eye-specific clusters of thalamic afferent boutons that create the ocular dominance columns, for example. Thus, quite simple rules of connectivity could generate the circuits that display the exquisite functional organization seen with the microelectrode and optical imaging.

Acknowledgments

This work was supported by EU grant (*QULG*3–1999–01064) and HFSP grant (*RG*0123/2000–B) to KACM.

References

AHMED, B., ANDERSON, J. C., DOUGLAS, R. J., MARTIN, K. A. C. & NELSON, J. C. (1994) Polyneuronal innervation of spiny stellate neurons in cat visual cortex. *Journal of Comparative Neurology* **341**, 39–49.

AHMED, B., ANDERSON, J. C., MARTIN, K. A. C. & NELSON, J. C. (1997) Map of the synapses onto layer 4 basket cells of the primary visual cortex of the cat. *Journal of Comparative Neurology* **380**, 230–242.

AMIR, Y., HAREL, M. & MALACH, R. (1993) Cortical hierarchy reflected in the organization of intrinsic connections in macaque monkey visual cortex. *Journal of Comparative Neurology* **334**, 19–46.

ANDERSON, J. C., DOUGLAS, R. J., MARTIN, K. A. C. & NELSON, J. C. (1994) Synaptic output of physiologically identified spiny stellate neurons in cat

visual cortex. *Journal of Comparative Neurology* **341**, 16–24.

ANDERSON, J. C. & MARTIN, K. A. C. (2001) Does bouton morphology optimize axon length? *Nature Neuroscience* **4**, 1166–1167.

BEAULIEU, C. & COLONNIER, M. (1983) The number of neurons in the different laminae of the binocular and monocular regions of area 17 in the cat. *Journal of Comparative Neurology* **217**, 337–344.

BRAITENBERG, V. & SCHÜZ, A. (1991) *Anatomy of the Cortex*. Berlin: Springer-Verlag.

CAJAL, S. R. Y. (1989) *Recollections of My Life*. Cambridge, MA: MIT Press.

CHERNIAK, C. (1992) Local optimization of neuron arbors. *Biological Cybernetics* **66**, 503–510.

COX, D. R. & ISHAM, V. (1980) *Point Processes. Monographs on Applied Probability and Statistics*. London, New York: Chapman and Hall.

CREUTZFELDT, O. D. (1977) Generality of the functional structure of the neocortex. *Naturwissenschaften* **64**, 507–517.

DANTZKER, J. L. & CALLAWAY, E. M. (2000) Laminar sources of synaptic input to cortical inhibitory interneurons and pyramidal neurons. *Nature Neuroscience* **3**, 701–707.

DOUGLAS, R. J., KOCH, C. K., MAHOWALD, M., MARTIN, K. A. C. & SUAREZ, H. H. (1995) Recurrent excitation in neocortical circuits. *Science* **269**, 981–985.

DOUGLAS, R. J., MARTIN, K. A. C. & WHITTERIDGE, D. (1991) An intracellular analysis of the visual responses of neurons in cat visual cortex. *Journal of Physiology (London)* **440**, 659–696.

EFRON, B. & TIBSHIRANI, R. J. (1993) An Introduction to the Bootstrap, Vol. 57 of *Monographs on Statistics and Applied Probability*. New York: Chapman and Hall.

ENGERT, F. & BONHOEFFER, T. (1999) Dendritic spine changes associated with hippocampal long-term synaptic plasticity. *Nature* **399**, 66–70.

FELDMEYER, D. & SAKMANN, B. (2000) Synaptic efficacy and reliability of excitatory connections between the principal neurons of the input (layer 4) and the output (layer 5) of the neocortex. *Journal of Physiology* **525**, 31–39.

FELLER, W. (1971) *An Introduction to Probability Theory and Its Applications II. Wiley Series in Probability and Mathematical Statistics*. John Wiley and Sons.

FREEMAN, W. J. (1975) Mass action in the nervous system. New York: Academic Press.

FREUND, T. F., MAGLÓCZKY, Z., SOLTESZ, I. & SOMOGYI, P. (1986) Synaptic connections, axonal and dendritic patterns of neurons immunoreactive for cholecystokinin in the visual cortex of the cat. *Neuroscience* **19**, 1133–1159.

FREUND, T. F., MARTIN, K. A. C., SMITH, A. D. & SOMOGYI, P. (1983) Glutamate decarboxylaseimmunoreative terminals of Golgi-impregnated axo-axonic cells of presumed basket cells in synaptic contact with pyramidal neurons of the cat's visual cortex. *Journal of Comparative Neurology* **221**, 263–278.

FREUND, T. F., MARTIN, K. A. C. & WHITTERIDGE, D. (1985a) Innervation of cat visual areas 17 and 18 by physiologically identified X- and Y-type thalamic afferents. I. Arborization patterns and quantitative distribution of postsynaptic elements. *Journal of Comparative Neurology* **342**, 263–274.

FREUND, T. F., MARTIN, K. A. C. & WHITTERIDGE, D. (1985b) Innervation of cat visual areas 17 and 18 by physiologically identified X- and Y-type thalamic afferents. II. Identification of postsynaptic targets by GABA immunocytochemistry and Golgi impregnation. *Journal of Comparative Neurology* **342**, 263–274.

FRIEDLANDER, M. J. & MARTIN, K. A. C. (1989) Development of Y-axon innervation of cortical area 18 in the cat. *Journal of Physiology (London)* **416**, 183–213.

FRIEDLANDER, M. J. & STANFORD, L. R. (1984) Effects of monocular deprivation on the distribution of cell types in the LGN_d: A sampling study with fine-tipped micropipettes. *Experimental Brain Research* **53**, 451–461.

GABBOTT, P. L. A., MARTIN, K. A. C. & WHITTERIDGE, D. (1987) Connections between pyramidal neurons in layer 5 of cat visual cortex (area17). *Journal of Comparative Neurology* **259**, 364–381.

GAREY, L. J. & POWELL, T. P. (1971) An experimental study of the termination of the lateral geniculo-cortical pathway in the cat and monkey. *Proceedings of the Royal Society of London. Series B. Biological sciences* **179**, 41–63.

GILBERT, C. D. & WIESEL, T. N. (1983) Clustered intrinsic connections in cat visual cortex. *Journal of Neuroscience* **3**, 1116–1133.

GONCHAR, Y., TURNEY, S., PRICE, J. L. & BURKHALTER, A. (2002) Axo-axonic synapses formed by somatostatin-expressing GABAergic neurons in rat and monkey visual cortex. *Journal of Comparative Neurology* **443**, 1–14.

HELLWIG, B., SCHÜZ, A. & AERSTSEN, A. (1994) Synapses on axon collaterals of pyramidal cells are spaced at random intervals: A Golgi study in the mouse cerebral cortex. *Biological Cybernetics* **71**, 1–12.

HUBEL, D. H. & WIESEL, T. N. (1962) Receptive fields, binocular interaction and functional architecture in the cat's visual cortex. *Journal of Physiology (London)* **160**, 106–154.

HUBEL, D. H. & WIESEL, T. N. (1965) Receptive fields and functional architecture in two nonstriate visual areas (18 and 19) of the cat. *Journal of Neurophysiology* **28**, 229–289.

HUBEL, D. H. & WIESEL, T. N. (1972) Laminar and columnar distribution of geniculo-cortical fibers in the macaque monkey. *Journal of Comparative Neurology* **146**, 421–450.

KISVÁRDAY, Z. F., MARTIN, K. A. C., FREUND, T. F., MAGLÓCZKY, Z. S., WHITTERIDGE, D. & SOMOGYI, P. (1986) Synaptic targets of HRP-filled layer III pyramidal cells in the cat striate cortex. *Experimental Brain Research* **64**, 541–552.

KISVÁRDAY, Z. F., MARTIN, K. A. C., FRIEDLANDER, M. J. & SOMOGYI, P. (1987) Evidence for interlaminar inhibitory circuits in striate cortex of cat. *Journal of Comparative Neurology* **260**, 1–19.

KISVÁRDAY, Z. F., MARTIN, K. A. C., WHITTERIDGE, D. & SOMOGYI, P. (1985) Synaptic connections of intracellularly filled clutch neurons: A type of small basket neuron in the visual cortex of the cat. *Journal of Comparative Neurology* **241**, 111–137.

KOZLOSKI, J., HAMZEI-SICHANI, F. & YUSTE, R. (2001) Stereotyped position of local synaptic targets in neocortex. *Science* **293**, 868–872.

LEVAY, S. (1986) Synaptic organisation of claustral and geniculate afferents to the visual cortex of the cat. *Journal of Neuroscience* **6**, 3564–3575.

LORENTE DE NÓ, R. (1949) Cerebral cortex: Architecture, intracortical connections, motor projections. In *Physiology of the Nervous System* (edited by FULTON, J.) pp. 288–313. New York: Oxford University Press.

MALETIC-SAVATIC, M., MALINOW, R. & SVOBODA, K. (1999) Rapid dendritic morphogenesis in CA1 hippocampal dendrites induced by synaptic activity. *Science* **283**, 1923–1927.

MARTIN, K. A. C. & WHITTERIDGE, D. (1984) Form, function and intracortical projections of neurones in the striate visual cortex of the cat. *Journal of Physiology (London)* **353**, 463–504.

McGUIRE, B. A., HORNUNG, J. P., GILBERT, C. & WIESEL, T. N. (1984) Patterns of synaptic input to layer 4 of cat striate cortex. *Journal of Neuroscience* **4**, 3021–3033.

MITCHISON, G. (1991) Neuronal branching patterns and the economy of cortical wiring. *Proceedings of the Royal Society of London. Series B. Biological sciences* **245**, 151–158.

MULLER, W. & CONNOR, J. A. (1991) Dendritic spines as individual neuronal compartments for synaptic Ca^{2+} responses. *Nature* **354**, 73–76.

PETERS, A. & KAISERMAN-ABRAMOF, I. R. (1970) The small pyramidal neuron of the rat cerebral cortex. the perikaryon, dendrites and spines. *American Journal of Anatomy* **127**, 321–356.

PRESS, W. H., TEUKOLSKY, S. A., VETTERLING, W. T. & FLANNERY, B. P. (1997) *Numerical Recipes in C*. Cambridge: Cambridge University Press.

REID, R. C. & ALONSO, J. M. (1995) Specificity of monosynaptic connections from thalamus to visual cortex. *Nature* **378**, 281–284.

ROCKEL, A. J., HIORNS, R. W. & POWELL, T. P. S. (1980) The basic uniformity in structure of the neocortex. *Brain* **103**, 221–244.

ROCKLAND, K. S. & KNUTSON, T. (2001) Axon collaterals of Meynert cells diverge over large portions of area V1 in the macaque monkey. *Journal of Comparative Neurology* **441**, 134–147.

SHOLL, D. A. (1956) *The Organization of the Cerebral Cortex*. London: Methuen.

SILBERBERG, G., GUPTA, A. & MARKRAM, H. (2002) Stereotypy in neocortical microcircuits. *Trends in Neurosciences* **25**, 227–230.

SOMOGYI, P. (1989) Synaptic organization of GABAergic neurons and GABAa receptors in the lateral geniculate nucleus and visual cortex. In *Neural Mechanisms of Visual Perception* (edited by LAM, D. K. & GILBERT, C. D.) pp. 35–62. Portfolio Publishing.

SOMOGYI, P. & COWEY, A. (1981) Combined Golgi and electron microscopy study on the synapses formed by double bouquet cells in the visual cortex of the cat and monkey. *Journal of Comparative Neurology* **195**, 547–566.

SOMOGYI, P., KISVÁRDAY, Z. F., MARTIN, K. A. C. & WHITTERIDGE, D. (1983) Synaptic connections of morphologically identified and physiologically characterized large basket cells in the striate cortex of the cat. *Neuroscience* **10**, 261–294.

SOMOGYI, P., TÁMAS, G., LUJAN, R. & BUHL, E. H. (1998) Salient features of synaptic organisation in the cerebral cortex. *Brain Research. Brain Research Reviews* **26**, 113–135.

STRAHLER, A. N. (1957) Quantitative analysis of watershed geomorphology. *Transactions of the American Geophysical Union* **38**, 913–920.

SWINDALE, N. V. (1981) Dendritic spines only connect. *Trends in Neurosciences* **4**, 240–241.

SZENTÁGOTHAI, J. (1975) The 'module-concept' in cerebral cortex architecture. *Brain Research* **95**, 475–496.

TAMÁS, G., BUHL, E. H. & SOMOGYI, P. (1997) Fast IPSPs elicited via multiple synaptic release sites by different types of GABAergic neurones in the cat visual cortex. *Journal of Physiology (London)* **500**, 715–738.

TAMÁS, G., SOMOGYI, P. & BUHL, E. H. (1998) Differentially interconnected networks of GABAergic interneurons in the visual cortex of the cat. *Journal of Neuroscience* **18**, 4255–4270.

TANAKA, K. (1983) Cross-correlation analysis of geniculostriate neuronal relationships in cats. *Journal of Neurophysiology* **49**, 1303–1318.

TETTONI, L., GHEORGHITA-BAECHLER, F., BRESSOUD, R., WELKER, E. & INNOCENTI, G. M. (1998) Constant and variable aspects of axonal phenotype in cerebral cortex. *Cerebral Cortex* **8**, 543–552.

WHITE, E. L. (1989) *Cortical Circuits: Synaptic Organization of the Cerebral Cortex. Structure, Function, and Theory*. Boston, Basel: Birkhäuser.

WINFIELD, D. A. & POWELL, T. P. (1983) Laminar cell counts and geniculo-cortical boutons in area 17 of cat and monkey. *Brain Research* **277**, 223–229.

WINFIELD, D. A., RIVERA-DOMINGUEZ, M. & POWELL, T. P. S. (1981) The number and distribution of Meynert cells in area 17 of the macaque monkey. *Proceedings of the Royal Society of London. Series B. Biological Sciences* **213**, 27–40.